CONTENT BASED IMAGE RETRIEVAL: THE FOUNDATION FOR FUTURE CASE-BASED AND EVIDENCE-BASED OPHTHALMOLOGY

Scott T. Acton[1], Peter Soliz[2,3], Stephen Russell[3], Marios S. Pattichis[4]

[1]Depts. of Electrical & Computer Engineering, Biomedical Engineering, University of Virginia, USA
[2]VisionQuest, Albuquerque, New Mexico, USA
[3]Dept. of Ophthalmology, University of Iowa, Iowa City, Iowa, USA
[4]Dept. of Electrical & Computer Engineering, University of New Mexico, USA
{acton@virginia.edu, pattichis@ece.unm.edu, psoliz@visionquest-bio.com}

ABSTRACT

For medical and epidemiologic investigators and caregivers, one powerful functionality yet to be developed is the ability to group retinal images based upon common pathologic appearance. Such a tool would enable advances in evidence-based medicine and would accelerate automated or computer-assisted screening and diagnosis. In this report, we show that current, traditional content based image retrieval methods are insufficient to sort dichotomous images (age-related macular degeneration and Stargardt disease) and then propose novel feature extraction techniques that may improve retrieval performance. Prior to processing of the images, a specialized diffusion method to enhance the contrast, reduce the discontinuity, and eliminate edge artifacts is applied to facilitate segmentation. A robust statistic is applied to find abnormal areas and to differentiate AMD from SD. Two methods of analyzing the subretinal deposits are presented – a granulometry based on area morphology and an AM-FM model. Preliminary data show that the image analysis tools show promise as a useful retrieval tool.

Index Terms: Image analysis, content based image retrieval, retinal imaging, ophthalmology, phenotyping.

1. INTRODUCTION

1.1 Background

Previously, content based medical image retrieval has been considered for the use in the Picture Archival and Communications System (PACS), [1] and other applications requiring access to large databases of digital medical images [2]. For example, the Image Retrieval in Medical Applications (IRMA) and the Automatic Search and Selection Engine with Retrieval Tools (ASSERT) system for use on High Resolution Lung CT images (HRCT) have been considered for use as diagnostic aids [3] [4]. For the most part, these systems have been used primarily in research for feature analysis; however, clinical implementations have not as yet taken place [5].

1.2 Significance

Future medical information systems will be instrumental in providing enhanced medical care with significant reduction in costs. To aid in the clinical decision making process, it will be necessary to search large image databases for images with similar pathologic appearances or anatomical features, locate images taken using other modalities, and display these images in a manner that will rapidly provide the physician the most significant information possible. Though, today's medical information systems provide some image search capabilities, annotated images have proven to contain error rates of up to 16% in identifying even the correct anatomical region [6].

This paper presents methods that may enable evidence-based medicine and case-based reasoning to improve healthcare. The requirements in evidence-based medicine will likely benefit from automated retrieval of medical images. The clinical benefit in eye care of a CBIR has not been explored and while the critical requirements for a medical image retrieval system have not been defined, the potential clinical and research benefits in ophthalmology are clear.

1.2 Importance of Age-related Macular Degeneration

Age-related macular degeneration (AMD) is the most common cause of global visual loss and consists of a genetically heterogeneous group of disorders characterized by the development of subretinal yellow deposits called drusen. Approximately 1 out of every 3 Americans will develop this disorder by age 65. AMD in its advances stages may profoundly damage the central retina that subserves central vision. In the later stages, AMD may lead to complete loss of central vision resulting in legal blindness.

1.3 Pathological Features of AMD

There are a number of ocular features that may be used to categorize the type or predict the progression of AMD. The hallmark of the disorder is the drusen deposit which in early AMD, Small round or ovoid white or yellow-white deposits

beneath the retina, typically most visible in the central retina called the macula. In more advanced AMD drusen may become larger and may develop less distinct edges, often referred to as "soft" drusen. Other fundus features include regions of retinal pigment epithelial (RPE) hypo- and hyperpigmentation., Spatial location and the area affected are important indicators for diagnosis and prognosis and must be considered when developing a computer-based retrieval system. The later stages of AMD are characterized by localized regions of RPE cell loss (geographic atrophy) and by the growth of new blood vessels from the choroid that breach Bruch's membrane and elevate the retina, called choroidal neovascularization (CNV). Ideally, each of these features must be identified, along with their surface location on the retina, and spatial extent, in order to achieve a useful image retrieval system.

2. TRADITIONAL CBIR METHODS

Our first attempt to retrieve retinal images of similar pathology is based on traditional content based image retrieval (CBIR) methods. The traditional features used in CBIR are color, texture, and shape. As all of the retinal images have the same dominant shape (the near-circular perimeter of the retinal fundus picture), we will concentrate on color and texture measures. A complete review of past CBIR methods and a description of the basic CBIR engine have been given previously [**Error! Bookmark not defined.**].

2.1. Color Extraction

For color extraction, we utilize the hue-saturation-value (HSV) space because it separates hue information from intensity information. This differentiation is valuable in analyzing the pigmentation in the retinal images. For each image in the database, normalized HSV histograms are generated with 256 bins. The match measure for color is assessed by way of histogram intersection [**Error! Bookmark not defined.**].

2.2. Texture Extraction via Wavelets

For the traditional texture analysis, we elected to use 2D Haar wavelet decomposition. First, the three image planes of the HSV image are resized to a standard size of 128x128. Then, a 2D Haar decomposition yields 16384 coefficients. The top C coefficients in terms of magnitude are retained (C=60 in this application). Two coefficients are said to match (between two images) if they ageee in location and sign.

The match measure, as previously described in [7], penalizes deviation from the average (d.c.) value of the three HSV components. The a.c. terms are then matched to generate a normalized score that can be combined linearly with the color match measure.

2.3. Traditional CBIR Results

To evaluate the efficacy of the histogram-based color measure and the wavelet-based texture measure for the retinal image application, we constructed a ground truth database of 200 images. The 200 images were manually classified by an ophthalmologist at the University of Iowa and represent characteristic examples of either AMD or Stargardt's disease (SD). The AMD images were further grouped into 12 subjective phenotypes (where possible) based upon similarity of the fundus' appearance, as determined by our retinal specialist.

We tested the combined color/texture measures, the color measure and the wavelet-based texture measure in retrieving images of SD or AMD. With a best case performance shown in of approximately 2/3 correct retrieval, the color and texture features are incapable of accurately determining the difference between SD and AMD in a dichotomous sort.

The performance for locating images of the same subclass using these traditional measures was abysmal with an average retrieval precision below 30%. Such a retrieval tool would not be useful clinically.

3. SPECIALIZED METHODS FOR RETINAL IMAGES

The results from traditional CBIR reveal that these basic feature extraction methods are not sufficient for the retinal image application. Here, in Section 3, we present novel methodology that shows promise for generating a richer set of features for sorting or retrieving images of similar disease but minimal dissimilarities of appearance. The methods include a speckle reducing anisotropic diffusion step used for enhancement, a method to find regions of severe abnormality (atrophy) from SD, a specialized granulometery which distinguish drusen deposits in AMD, and an AM-FM approach to characterizing local texture.

3.1. Enhancement via Speckle Reducing Anisotropic Diffusion

The imaging apparatus used here to image the retina is subject to speckle artifact. One goal, in our analysis, is to remove the features caused by speckle so that the disease-related features (i.e., the subretinal deposits such as drusen in AMD or concentric annular atrophy and pisciform deposits in SD) can be extracted and localized.

We propose the use of speckle reducing anisotropic diffusion (SRAD) for enhancement that precedes segmentation and feature extraction. One may consider basic anisotropic diffusion the gradient-sensitive version of isotropic smoothing. In the same manner, SRAD is sensitive to the coefficient of variation locally, preserving edges and boundaries in the presence of signal-dependent speckle. SRAD is based on a discretized operator that yields a local coefficient of variation that we call the *instantaneous*

coefficient of variation, which is a local approximation of the ratio between standard deviation of intensity and mean intensity, as derived in [8].

In SRAD, the output image $I(x,y;T)$ is evolved according to the following PDE:

$$\partial I(x,y;T)/\partial t = div\left[c(q)\nabla I(x,y;T)\right] \qquad (1)$$

where ∇ is the gradient operator and *div* the divergence operator. T is the update time for which $T=0$ denotes the original input image. The diffusion coefficient $c(q)$ is given by

$$c(q) = \left\{1 + \frac{\left[q^2(x,y;T) - q_0^2(T)\right]}{q_0^2(T)\left(1+q_0^2(T)\right)}\right\}^{-1} \qquad (2)$$

where $q(x,y;T)$ is the instantaneous coefficient of variation, $q_0(T)$ is the speckle noise level at update time T, which is determined by measuring the standard deviation of intensity over the mean in a homogeneous region. Equation (1) describes the enhancement of image I as an evolutionary, iterative process. An example SRAD result is shown in Figure 1. Having enhanced considerably the quality of the images through this process, the application of the AM-FM techniques to extract features is significantly improved.

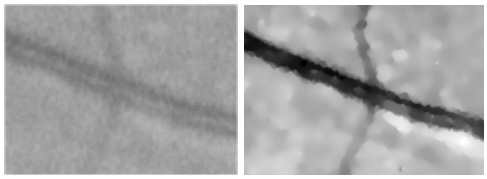

Fig. 1: Original intensity band of retinal image subsection (left) and SRAD-enhanced result (right).

3.2. Stargardt's Disease Detection

In the later stages of Stargardt's disease, images contain large concentric, annular regions of atrophy of the RPE about the fovea (Figure 2). To differentiate these images from AMD images, we have attempted to detect such regions of abnormality. Our approach commences with the SRAD enhancement and then uses a method called Gradient Inverse Coefficient of Variation (GICOV) to detect circular or elliptical regions of strong contrast. The GICOV statistic depends upon an initial elliptical regression on an edge map, which we create using the SRAD-enhanced image.

Let $(X(s), Y(s))$ represent a 2D smooth closed contour parameterized by $s \in [0, 1]$. If $I(x, y)$ denotes an image then the mean of the image gradient over the entire contour computed in the outward normal direction is given by

$$M(X,Y) = \frac{1}{L}\int_0^1 \nabla I(X(s),Y(s)) \cdot \mathbf{n}(X(s),Y(s))\, ds, \quad (3)$$

where $\mathbf{n}(X(s), Y(s))$ is the unit outward normal to the contour at $(X(s),Y(s))$ and L is the length of the contour. Likewise, the variance of the image gradient over the entire contour computed in the outward normal direction $\mathbf{n}$ is given by

$$S^2(X,Y) = \frac{1}{L}\int_0^1 \left[\nabla I(X(s),Y(s)) \cdot \mathbf{n}(X(s),Y(s))\right]^2 ds - M^2(X,Y). \quad (4)$$

The GICOV score is the length-normalized ratio between (3) and (4). Such a score is high where magnitude of the gradient is high around the contour and the contour gradient magnitude has a low variance. This statistic enables the extraction of the degenerated regions.

Fig. 2 shows an example result, wherein testing with our 200-image database, the accuracy of extracting the 100 Stargardt's images is 63.5%, which is greater than the results obtained by the traditional approach (for Q=100), but is not acceptable clinically. We plan to combine this GICOV based detection with the AM-FM features for more robust detection of Stargardt's disease.

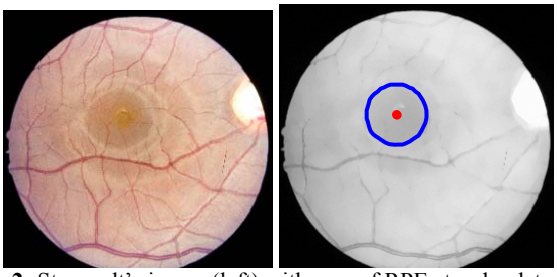

Fig. 2: Stargardt's image (left) with area of RPE atrophy detected correctly by GICOV method (right).

3.3. Drusen Detection

Determination of the location and size of drusen are critical to automated diagnosis and retrieval of similar AMD images (See Fig. 3 for an example image region). We are pursuing two fundamentally different approaches to detecting and characterizing drusen: an area morphology- based granulometry and an AM-FM model.

The granulometry approach begins with an SRAD-enhanced image so that speckle artifact does not confound detection of drusen (as shown in Fig. 4 (left)). This particular granulometry technique uses an area open operation [9] instead of the conventional opening operator. An area opening function removes all connected components in all binary level sets of the image with an area less than that prescribed. The difference between two area openings yields the drusen detection result shown in Fig. 4 (right).

3.4. Drusen Characterization via AM-FM Model

For AM-FM modeling, we use dominant component analysis (DCA) [10]. In DCA, an image is first filtered through a multiscale filterbank. At every pixels, we select the channel with the strongest magnitude response and apply AM-FM demodulation to get [10]:

$$I(x,y) \cong a(x,y)\cos\phi(x,y). \qquad (5)$$

In equation (5), $a(x,y)$ is a positive, slowly-varying

amplitude function, $\phi(x,y)$ represents a phase function and $\nabla\phi(x,y)$ represents the instantaneous frequency.

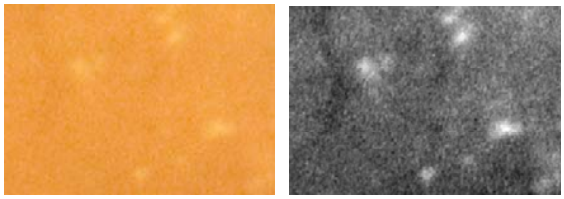

Fig. 3: Retinal region showing drusen. Color image (left) and green band (right).

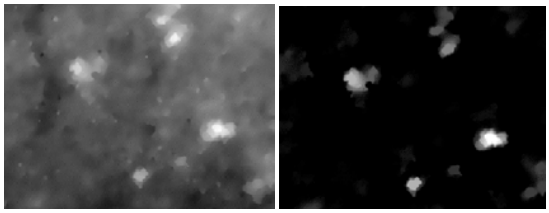

Fig. 4: SRAD result for Fig. 3 (left) and granulometry illustrating drusen result (right).

For segmenting drusen areas, we first compute the AM-FM dominant component and then process the amplitude and instantaneous frequency magnitude $\|\nabla\phi(x,y)\|$ to identify suspicious or presumptive regions. We then apply simple thresholding to identify moderately high probability regions with low instantaneous frequency magnitude.

By applying a threshold cutoff to the resulting amplitude component, we detect moderately bright regions (representing drusen) while rejecting darker blood vessel regions. Threshold cutoff by instantaneous frequency magnitude rejects noisy, high-frequency regions while also rejecting large, uniform intensity regions. From the remaining detected regions, we remove components that have low probability to represent features such as very small or very long components. (Here, we use the term small to refer to components with a small number of pixels. We also define components as being very long if either the ratio of the vertical to horizontal component is significantly above or below 1, for rectangular regions or if the ratio of the binary component bounding box to the area of the pixels is significantly above 1, for irregularly shaped long components.)

Typical results are shown in Fig. 5 (green channel only). In Fig. 5, we can see that that several moderately sized drusen regions are correctly detected. A clear example of a true positive is the 'Z' like pattern in the middle left of the image. A false positive example is seen in the middle right region, where a bright region is found near the blood vessels. It is also clear that there are many examples of suspected small, false negative regions. We also have an example of a bright false negative in the upper middle region.

We are currently attempting to include this rich AM-FM feature set in a content based retrieval engine.

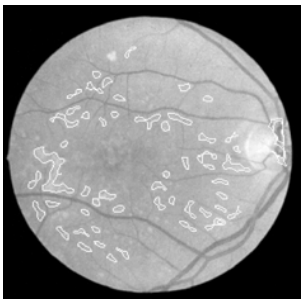

Fig. 5: Drusen feature detection using an AM-FM model.

4. CONCLUSION

This paper has summarized our initial efforts in the design of a content based retrieval engine for retinal images. Our studies show that the existing color histogram and wavelet tools are not currently capable of differentiating the subtleties of the various retinal pathologies. We have proposed special-purpose image analysis techniques that show promise in leading to a successful retrieval system.

REFERENCES

[1] E. El-Kwae, H. Xu, and M. R. Kabuka, "Content-based retrieval in picture archiving and communication systems," *Journal of Digital Imaging* 13(2), pp. 70-81, 2000.

[2] A. Rosset, O. Ratib, A. Geissbuhler, and J.-P. Vallfiee, "Integration of a multimedia teaching and reference database in a PACS environment," *RadioGraphics* 22(6), pp. 1567-1577, 2002.

[3] D. Keysers, J. Dahmen, H. Ney, B. B. Wein, and T. M. Lehmann, "A statistical framework for model{based image retrieval in medical applications," *Journal of Electronic Imaging* 12(1), pp. 59-68, 2003.

[4] C.-R. Shyu, C. E. Brodley, A. C. Kak, A. Kosaka, A. M. Aisen, and L. S. Broderick, "ASSERT: A physician-in-the-loop content-based retrieval system for HRCT image databases," *Computer Vision and Image Understanding*, 75, pp. 111-132, July/August 1999.

[5] E. El-Kwae, H. Xu, and M. R. Kabuka, "Content-based retrieval in picture archiving and communication systems," *Journal of Digital Imaging* 13(2), pp. 70-81, 2000.

[6] M. O. Gould, M. Kohnen, D. Keysers, H. Schubert, B. B. Wein, J. Bredno, T. M. Lehmann, "Quality of DICOM header information for image categorization," in: *International Symposium on Medical Imaging*, Vol. 4685 of SPIE Proceedings, San Diego, CA, USA, 2002, pp. 280-287.

[7] C. E. Jacobs, A. H. Finkelstein, and D. H. Salesin, "Fast multiresolution image querying," in *Proceedings of the 22nd annual conference on Computer graphics and interactive techniques*: ACM Press, 1995.

[8] Y. Yu and S.T. Acton, "Speckle reducing anisotropic diffusion," *IEEE Transactions on Image Processing*, vol. 11, pp. 1260-1270, 2002.

[9] S. T. Acton, "Fast algorithms for area morphology," *Digital Signal Processing*, vol. 11, pp. 187, 2001.

[10] V. Murray and M.S. Pattichis, "Robust Multiscale AM-FM Demodulation of Digital Images," in *Conf. 2007 IEEE Int. Conf. on Image Processing,* pp. 465-468, 2007.